Journal of Enhanced Heat Transfer, 18 (3): 191–207 (2011)

MODELS FOR PRESSURE DROP AND HEAT TRANSFER IN AIR COOLED COMPACT WAVY FIN HEAT EXCHANGERS

M. M. Awad & Y. S. Muzychka*

Faculty of Engineering and Applied Science, Memorial University of Newfoundland, St. John's, Newfoundland, Canada, A1B 3X5

*Address all correspondence to M. M. Awad E-mail: awad@engr.mun.ca

A detailed review and analysis of the thermal-hydrodynamic characteristics in air-cooled compact wavy fin heat exchangers is presented. New models are proposed which simplify the prediction of the Fanning friction factor f and the Colburn j factor. These new models are developed by combining the asymptotic behavior for the low Reynolds number and laminar boundary layer regions. In these two regions, the models are developed by taking into account the geometric variables such as: fin height (H), fin spacing (S), wave amplitude (A), fin wavelength (λ), Reynolds number (Re), and Prandtl number (Pr). The proposed models are compared with numerical and experimental data for air at different values of the geometric variables obtained from the published literature. The new models for f and j cover a wide range of the Reynolds number. Since the model is based analytically, it will also allow for proper design assessment of heat exchanger performance.

KEY WORDS: *compact heat exchangers, wavy fins, models, friction factor, Colburn factor, performance modeling*

1. INTRODUCTION

This paper, which contains three major sections, presents the results of a robust modeling approach for wavy fins. The first section gives a review of the data and correlations, which are presently available in the open literature. Next, a discussion on the development of a simple asymptotic model for the prediction of the Fanning friction factor (f) and the Colburn factor (j) for the wavy fin geometry is presented. Finally, a discussion of the proposed models and a comparison with published data for air is given.

The wavy fin geometry shown in Fig. 1 is widely used in air-cooled heat exchangers and heat sink systems. Fin waviness contributes to heat transfer enhancement by means of an increased surface area due to corrugations and turbulence promotion at larger flows. At moderate Reynolds numbers, re-circulation zones form periodically and provide enhancement by means of turbulent mixing of the fluid and boundary layer re-initiation.

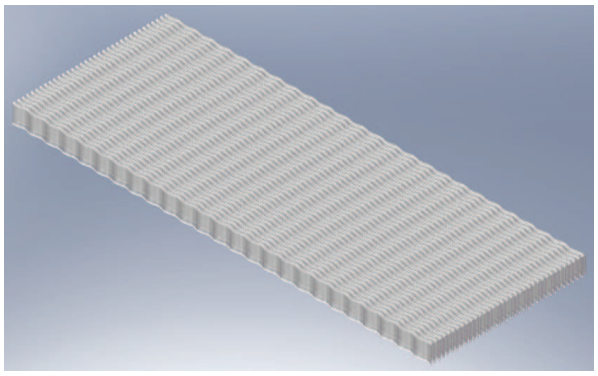

FIG. 1: Wavy fin geometry.

2. LITERATURE REVIEW

A number of previous studies investigating the thermal and hydraulic characteristics of the wavy fins have been reviewed for this work. While predominantly used with

1065–5131/11/$35.00

NOMENCLATURE

$2A$	twice the wavy fin amplitude, m
c_p	heat capacity, J/kg.K
D_h	hydraulic diameter, m
e	error
$E(\cdot)$	complete elliptic integral second kind
f	Fanning friction factor, = $\tau_m/(0.5\rho_m u_m^2)$
H	fin height, m
h	heat-transfer coefficient, W/m^2·K
j	Colburn factor, = StPr$^{2/3}$
K	consistency index, kg/m.s^{2-n}
k	thermal conductivity, W/m·K
L	channel length, m
L^+	dimensionless hydrodynamic entrance length, = $L/D_h\mathrm{Re}_{Dh}$
L_d	wavy fin length, m
L_e	effective length, m
n	power-law index
Nu	Nusselt number, = hD_h/k
Pr	Prandtl number, = $\mu c_p/k$
Re	Reynolds number, = $\rho u_m D_h/\mu$
Re$_g$	generalized Reynolds number, = $\rho u_m^{2-n} D_h^n/K$
RH	relative humidity
r_h	hydraulic radius, m
S	fin pitch, m
St	Stanton number, = Nu/(RePr)
t	fin thickness, m
u_m	mean velocity, m/s

Greek Symbols

α	cross-section aspect ratio, = (S/H)
ε	wavy-fin-channel spacing ratio, = $(S/2A)$
γ	wavy-fin-channel corrugation ratio, = $(2A/\lambda)$
λ	wavy fin wavelength, m
μ	dynamic viscosity, N·s/m^2
θ	corrugation angle, $^\circ$
ρ	fluid density, kg/m^3
τ	wall shear stress, N/m^2

Subscripts

app	apparent
asy	asymptotic
b	bulk value
channel	channel
D_h	based on hydraulic diameter
H1	uniform heat flux boundary condition
m	mean
T	constant wall temperature boundary condition
w	at wall conditions
wavy	wavy fin

Acronyms

CFD	computational fluid dynamics
FPI	fin per inch
LBL	laminar boundary layer
NTU	number of transfer units
OSF	offset strip fin
RMS	root-mean-square error

air as a working fluid, few studies have addressed issues with liquids. Early data on wavy fin geometries can be found in Kays and London (1984) for three sets of geometric parameters using air as a working fluid. These geometries had (fins per inch) FPI = 11.4, 11.5, and 17.8, respectively with λ = 0.375 in (9.525 mm).

Goldstein and Sparrow (1977) studied corrugated channels with triangular waves. Although triangular waves were somewhat different from sinusoidal waves, many flow features were common to both triangular waves and sinusoidal waves. They were among the first to provide detailed data on triangular waves. They carried out experiments based on the naphthalene sublimation technique to determine the local and average transfer characteristics for flow in a corrugated wall channel. The range of their experiments encompassed the laminar, transition, and low-Reynolds-number turbulent regimes (Re = 150–2000). They used two corrugation cycles (two wavelengths). They measured local mass transfer in the spanwise (i.e., cross stream) and streamwise directions. They also determined overall transfer rates. The experiments demonstrated the presence of different complex transport processes and related fluid flow phenomena. These included secondary flows and associated spanwise mass transfer variations, suppression of the secondary flow by counteracting centrifugal forces, and destruction of the secondary flow by the onset of turbulence. Flow separation on the leeward faces of the corrugated wall caused

a sharp decrease in the local transfer rates, but relatively high transfer rates were in evidence in the reattachment region. In the laminar range, they found that the average transfer coefficients for the corrugated wall channel were only moderately larger than those for a parallel-plate channel. On the other hand, in the low-Reynolds-number turbulent regime, they found that the average transfer coefficients for the corrugated wall channel were about three times larger than those for a parallel-plate channel, but there was an even greater penalty in pumping power.

O'Brien and Sparrow (1982) performed experiments to determine forced convection heat-transfer coefficients and friction factors for flow in a corrugated duct. The corrugation angle was 30° and the inter wall spacing was equal to the corrugation height. The range of the Reynolds number, based on the duct hydraulic diameter was from 1500 to 25000, and the range of the Prandtl number was from 4 to 8 by varying the temperature level of water. Flow visualization, using the oil-lampblack technique, revealed a highly complex flow pattern, including large zones of recirculation adjacent to the rearward-facing corrugation facets. Their heat transfer correlation was

$$\mathrm{Nu} = 0.409\mathrm{Re}^{0.614}\mathrm{Pr}^{0.34} \tag{1}$$

In the above equation, the 0.614 value of the Reynolds number exponent was low when compared to the 0.8 exponent for a standard turbulent duct flow situation because the corrugated duct flow had large zones of recirculation not present in conventional duct flows. The 0.34 value of the Prandtl number exponent in Eq. (1) was intermediate with respect to other values found in the literature for turbulent flows that ranged from 0.3 to 0.4 with an exponent of 1/3 being quite common in the literature. The enhancement of heat transfer as compared to a conventional parallel-plate channel was about a factor of 2.5. Friction factors obtained from measured axial pressure distributions were virtually independent of the Reynolds number and equal to 0.57, a value appreciably greater than that for unidirectional duct flows.

Sparrow and Comb (1983) measured heat transfer, pressure drop, and observed fluid flow experimentally for water flowing in a corrugated-wall duct. They gave consideration to the effects of varying the spacing between the corrugated walls and of different fluid flow inlet conditions. Also, they examined the role of the noncorrugated sidewalls in the evaluation of the heat-transfer coefficient. Using the a least-square fit of the experimental data, the fitted equation in a power law form was given by

$$\mathrm{Nu} = 0.491\mathrm{Re}^{0.632}\mathrm{Pr}^{0.3} \tag{2}$$

They carried out performance evaluations for different constraints — fixed pumping power, fixed pressure drop, and fixed mass flow. For these three cases, they found that the heat-transfer coefficient for the larger interwall spacing was slightly lower than that for the smaller interwall spacing, but the pressure drop was also lower.

Sparrow and Hossfeld (1984) performed experiments to determine the heat transfer, pressure drop, and flow field responses to the rounding of the peaks of a corrugated-wall duct. They used two different degrees of corrugation-peak roundedness in addition to sharp (i.e., unrounded) corrugation peaks. In their experiments, the range of the Reynolds number was from 2000 to 33,000 while the range of the Prandtl number was from 4 to 11 by varying the temperature level of water. At a given Reynolds number (i.e., given mass flow rate), they found that the rounding of the corrugation peaks brought about a decrease in the Nusselt number that was accentuated at larger Reynolds numbers. The friction factor corresponding to a given Reynolds number decreased even more than the Nusselt number. On the other hand, at equal pumping power, the Nusselt number was relatively insensitive to whether the peaks were rounded or sharp. Flow visualization experiments showed that rounding reduced the size of the separated region that was spawned at each corrugation peak.

Amano (1985) reported a numerical study on hydrodynamic and heat transfer characteristics in a periodically corrugated wall channel for both laminar and turbulent flows. He based the solution method of the governing transport equations on the modified hybrid scheme. As a result of extensive computations, he clarified the complex flow patterns in the perpendicular corrugated wall channel and explained the mechanisms of heat transfer relating to the flow phenomena of separation, deflection, recirculation, and reattachment. Finally, he observed that the effect of the step ratio on the local Nusselt number was minor. Moreover, he found that both skin friction and heat transfer patterns changed drastically from laminar to turbulent flows.

Amano et al. (1987) performed a numerical study examining flow and heat transfer characteristics in a channel with periodically corrugated walls. They demonstrated the complexity of the flow in this type of channels by such phenomena as flow impingement on the walls, separation at the bend corners, flow reattachment and flow recirculation. Because of the strong non-isotropic nature of the turbulent flow in the channel, they employed the full Reynolds-stress model for the evaluation of turbulence quantities. They made computations for several different

corrugation periods and for different Reynolds numbers. The results computed by using the present model showed excellent agreement with experimental data for mean velocities, the Reynolds stresses, and average Nusselt numbers.

Asako and Faghri (1987) developed a finite volume methodology to predict two-dimensional ($\alpha \rightarrow 0$) fully developed heat-transfer coefficients, friction factors, and streamlines for flow in a corrugated duct with sharp corner in the laminar flow regime ($100 \leq \mathrm{Re} \leq 1000$). The wall had a triangular profile and was maintained at a uniform temperature. The basis of their method was an algebraic coordinate transformation that mapped the complex fluid domain onto a rectangle. This method could be adopted for other convection-diffusion problems in which two boundaries of the flow domain did not lie along the coordinate lines. They found representative results for laminar flow, uniform wall temperature, and for a range of the Reynolds number, Prandtl number, corrugation angle, and dimensionless interwall spacing. The streamlines showed that the flow patterns were highly complex including large recirculation zones. The pressure drops and friction factor results were higher than the corresponding values for a straight duct.

Asako et al. (1988) determined numerically heat transfer and pressure drop responses of a corrugated duct with rounded corners. They approximated the duct boundaries by a cosine function. They carried out computations for Pr of 0.7, in the Reynolds number range from 100 to 1000, for three assigned corrugation angles, and for four values of aspect ratios. They found that rounding of the corners resulted in a decrease of f and Nu. They compared heat transfer performance of a duct with rounded corners to a straight duct and to a duct with sharp corners under three different constraints: fixed pumping power, fixed pressure drop, and fixed mass flow. They found that the heat transfer rates decreased or increased depending on the specific conditions.

Ali and Ramadhyani (1992) performed experiments to study convective heat transfer in the entrance region of corrugated channels. They used water as the working fluid. They examined two channel spacings for a single corrugation angle of 20°. They varied the flow rate over the range $150 \leq \mathrm{Re} \leq 4000$. Flow visualization under low-Reynolds-number flow conditions suggested the existence of longitudinal vortices, while at somewhat higher Reynolds numbers; they revealed the presence of spanwise vortices. For $\mathrm{Re} > 1500$, they found that Nusselt numbers in the corrugated channels exceeded those in the parallel-plate channel by approximately 140% and 240% for the two channel spacings, the corresponding increases in friction factor being 130% and 280%. Performance evaluations under the criteria of equal mass flow rate, equal pumping power, and equal pressure drop per unit length established both the corrugated channels as superior to the parallel-plate channel in intensifying heat transfer.

Rush et al. (1999) investigated local heat transfer and flow behavior for laminar and transitional flows in sinusoidal wavy passages. The experimental geometry consisted of a channel with a 10:1 aspect ratio bounded by two wavy walls. The walls were from 12 to 14 wavelengths long. During their experiments, they varied the wave amplitude, phase angle, and wall-to-wall spacing. Using visualization methods, they characterized the flow field as steady or unsteady, with special attention directed toward detecting the onset of macroscopic mixing in the flow. They found the location of the onset of mixing to depend on the Reynolds number and channel geometry. Instabilities manifested near the channel exit at low Reynolds numbers ($\mathrm{Re} \sim 200$) and moved toward the channel entrance with increasing the Reynolds number. At moderate Reynolds numbers ($\mathrm{Re} \sim 800$), the mixing was evident throughout the channel in the flow visualization studies. The onset of macroscopic mixing was directly linked to significant increases in local heat transfer.

Metwally and Manglik (2000) investigated the enhanced heat transfer behavior of laminar shear-thinning, power-law fluid flows in sinusoidal corrugated-plate channels. With duct plates at uniform wall temperature, they considered periodically developed flows for a wide range of channel corrugation aspect ratio ($0 \leq \gamma \leq 1$), flow rates ($10 \leq \mathrm{Re}_g \leq 1500$), and pseudoplastic flow behavior indices (n = 0.5, 0.8, and 1.0). They presented typical velocity and temperature distributions, along with extended results for the isothermal friction factor f and Colburn factor j. They found that enhanced forced convection is strongly influenced by γ, and the flow field displayed two distinct regimes: undisturbed laminar or no-swirl and swirl flow regimes. In the no-swirl regime, they obtained a behavior similar to that in fully developed straight duct flows with no cross-stream disturbance. The shear-thinning nature of the fluid, however, decreased f and enhanced j. In the swirl regime, flow separation and reattachment in the corrugation troughs generated transverse vortices that grew with Re_g and γ. The transition to this regime was also seen to be dependent on Re_g, γ, and *n*, and in shear-thinning flows, it occurred at a lower Re_g. The combined effects of the corrugated plate geometry and non-Newtonian fluid rheology enhanced heat trans-

fer, as measured by the factor j/f, of over 3.3 times that in a flat-plate channel depending upon γ, n, and Re_g.

Muley et al. (2002) presented steady-state heat transfer and isothermal pressure drop results for a novel wavy-channel heat exchanger core. The wavy geometry had a corrugation aspect ratio ($\gamma = 2A/\lambda$) of 0.15 and duct aspect ratio ($\alpha = S/H$) of 0.4533. They obtained experimental measurements for the Colburn factor j and Fanning friction factor f for laminar flows ($70 \leq \mathrm{Re} \leq 830$) of water ($\mathrm{Pr} \sim 6$). In addition, they developed a computational fluid dynamics (CFD) model to simulate periodically developed laminar flows in the wavy channel using the control-volume based commercial code FLUENT. They found that the computational f and j predictions were in excellent agreement ($\pm 10\%$) with the experimental data. Local temperature and flow field simulations showed a complex effect of the channel geometry. Based on the experimental and numerical results, they devised f and j correlations for the wavy-core performance and design tradeoffs. Their f and j correlations for $\mathrm{Re} > 100$ were

$$f = 3.051\mathrm{Re}^{-0.6365} \tag{3}$$

$$j = 0.173\mathrm{Re}^{-0.385}\left(\frac{\mu_b}{\mu_w}\right)^{0.14} \tag{4}$$

It should be noted that their f and j correlations were valid only for the wavy duct with γ of 0.15 and α of 0.4533 used in their study. They claimed that the wavy channels provided 1.40 to 2.35 times higher j/f compared to an equivalent straight duct, and up to 4.3 times higher heat transfer for the fixed geometry and pumping power constraint.

Lin et al. (2002) conducted an experimental study reporting the airside performance of the herringbone wavy fin geometry in wet conditions. In the visualization of the condensate flow pattern, they saw a very special "locally dry" spot of the corrugation wavy channel with $\theta = 15^\circ$ and $S = 8.4$ mm. They related this phenomenon to the recirculation of the airflow across the apex. Conversely, this phenomenon was not so clearly seen either for a fin pitch of 2.6 mm with a corrugation angle of 15° or a corrugation angle of 25°. Flow visualization of the non-uniform distribution of the condensation in the facets resulted in a dependence between the axial length and the friction factor. Based on their test results, they developed airside performance in terms of the Nusselt number and Fanning friction factor for the present herringbone wavy fin geometry in wet conditions. Their correlations were

$$\mathrm{Nu} = 0.02656\mathrm{Re}^{0.92333}\left(\frac{S}{D_h}\right)^{2.5906}\theta^{0.47028}RH^{0.07773} \tag{5}$$

$$f = 0.02403\mathrm{Re}^{-0.41543}\left(\frac{S}{D_h}\right)^{-0.096529} \times \theta^{1.3385}RH^{-0.13035} \tag{6}$$

The mean deviations of the proposed correlations of Eqs. (5) and (6) were 2.52% and 4.81%, respectively.

Zhang et al. (2003) investigated enhanced heat transfer characteristics of low Reynolds number airflows in three-dimensional sinusoidal wavy plate-fin channels. For the computational simulation, they considered the following assumptions: steady state, constant property, periodically developed, laminar forced convection. They modeled the wavy fin by its two asymptotic limits of 100% fin efficiency that corresponding to the entire fin surface was at the same temperature and zero fin efficiency that corresponding to the entire fin surface (but not the base or the primary surface) was adiabatic. They solved the governing equations numerically using finite-volume techniques for a non-orthogonal, non-staggered grid. In their computations, they had four cases of different values of α and ε with a constant value of $\gamma = 0.267$. They presented computational results for velocity and temperature distribution, isothermal Fanning friction factor f and Colburn factor j for airflow rates in the range of $10 \leq \mathrm{Re} \leq 1\,500$. Also, they compared the numerical results with experimental data for two cases ($\alpha = 0.637$ and $\varepsilon = 0.803$ for the first and $\alpha = 0.241$ and $\varepsilon = 0.303$ for the second). They found that there was an excellent agreement for the two different wavy-fin geometries. In addition, they highlighted the effect of fin density (ε) on the flow behavior and the enhanced convection heat transfer. They observed that the flow behavior was highly dependent on the flow rate. At a low flow rate ($\mathrm{Re} < 100$), viscous forces were dominant and the flow behavior was similar to that in a straight rectangular channel with the wavy surface simply providing a longer flow path or residence time. At a higher flow rate ($\mathrm{Re} > 100$), they observed swirl flows consisting of multiple pairs of counter-rotating helical vortices. The swirl flow regime led to a higher momentum and energy transport. The fin geometry parameters α and ε had various and perhaps competing effects on the thermal-hydraulic performance. They found that the f and j factors decreased with increasing α while they increased with increasing ε. Nevertheless, increasing fin density (ε) tended to promote a relatively better (j/f) performance under swirl-flow conditions. They obtained the optimum performance (j/f) when $\varepsilon = 0.470$ (Case 3).

Vyas et al. (2004) presented experimental and computational characterization of swirl flow and heat transfer in a normally two-dimensional (plate separation to

width = 0.067), sinusoidal wavy channel with γ = 0.25 and ε = 1. They carried out the computational work using finite-volume techniques for a non-orthogonal non-staggered grid. In their experimental visualization, they obtained flow pattern photographs using injection of very fine aluminum dust (63 μm) in the flow field, illuminating it with a high-luminosity light sheet and capturing the image on a digital camera with a shutter speed of 0.125 sec. They found that at Re = 125, the flow was essentially streamline and contoured to the wall waviness. At Re $>$ 200, lateral recirculation, induced by wall curvature, set in through regions of the wavy channels. The swirl strength and spatial flow coverage increased with Re to produce temperature field which had sharper gradients at the wall with considerable thinning of the boundary layer and enhanced heat transfer.

Zhang et al. (2004) simulated numerically laminar forced convection in air (Pr = 0.7) in two-dimensional ($\alpha \rightarrow 0$) wavy-plate-fin channels with sinusoidal wall corrugations. For the computational simulation, they considered the following assumptions: constant property, and periodically developed flow in uniform wall temperature plate channels. They presented velocity and temperature fields, isothermal Fanning friction factor (f), and Colburn factor (j) for different flow rates ($10 \leq$ Re $\leq$ 1 000), wall-corrugation severity ($0.125 \leq \gamma \leq 0.5$), and fin spacing ($0.1 \leq \varepsilon \leq 3.0$). They found that lateral vortices or re-circulation cells developed in the wavy-wall troughs as the axial flow got separated downstream of the wall-corrugation peaks and re-attached upstream of the subsequent wall peak, and their strength and coverage was a function of Re, γ, and ε. As the plate separation decreased, however, viscous forces dominated and dampened the swirl; with very large ε, the effect of wall waviness diminished and the core fluid flowed largely undisturbed. The surface waviness-induced periodic disruption and thinning of boundary layers along with lateral swirl mixing produced high local heat fluxes near the wall peak regions. The overall heat-transfer coefficient increased many fold compared to that in flat-plate channels with relatively small increases in the pressure drop penalty. They obtained the optimum (j/f) enhancement in the swirl flow regime (Re $>$ 100) with $\gamma > 0$ and $1.0 \leq \varepsilon \leq 1.2$.

Manglik et al. (2005) considered steady forced convection in periodically developed low Reynolds number in the range of $10 \leq$ Re $\leq$ 1000 using air (Pr = 0.7) flows in three-dimensional wavy-plate-fin cores. Using finite-volume techniques for a non-orthogonal non-staggered grid, they obtained constant property computational solutions. Their results showed that the wavy-fin density had an effect on the velocity and temperature fields, isothermal Fanning friction factor f, and Colburn factor j. It was seen that the fin waviness induced the steady and spatially periodic growth and disruption of symmetric pairs of counter-rotating helical vortices in the wall-trough regions of the flow cross-section. The thermal boundary layers on the fin surface were thereby periodically interrupted, resulting in high local heat transfer near the recirculation zones. On the other hand, increasing fin density tended to dampen the recirculation and confine it. The extent of swirl increased with flow rate, when multiple pairs of helical vortices were formed. As a result, this significantly enhanced the overall heat-transfer coefficient as well as the pressure drop penalty, when compared to that in a straight channel of the same cross-section. They found that the relative surface area compactness as measured by the (j/f) performance or the area goodness factor nevertheless increased with fin density.

Webb and Kim (2005) summarized briefly much of the significant work in wavy channel analysis.

Muley et al. (2006) investigated experimentally and computationally enhanced forced-convective heat transfer behavior of air flows (Pr $\sim$ 0.7) in a compact heat exchanger with three-dimensional, sinusoidal-wavy-plate fins. They explored plate-fins with three different corrugation aspect ratio γ = ($2A/\lambda$) = 0.0667, 0.1333, and 0.2667. They presented experimental j and f measurements for flow rates in the range 500 $<$ Re $<$ 5000. Based on control-volume techniques, they obtained computational results for periodically-fully-developed flows with $10 \leq$ Re $\leq$ 1 000. The numerically simulated local temperature and flow field map showed the complex effect of corrugation aspect ratio γ, and the concomitant j and f predictions were in good agreement with experimental measurements. They found that both j and f increased with γ to reflect the relatively stronger flow recirculation in the wall-trough regions, and spatially more frequent periodic boundary-layer disruptions upstream of the corrugation peaks that enhance heat transfer in plate-fin channels. The relative enhancement, as measured by the Area Goodness Factor (j/f), however was found to be highest with γ = 0.0667.

Tao et al. (2007) presented a 3D numerical investigation of the air side performance of the wavy fin surface using body-fitted coordinates. Results for local Nusselt number distributions on the whole wavy fin and plain plate fin surfaces showed that the local Nusselt number decreased quickly along the flow direction and the values at the upstream were about 10 times of those at the down-

stream. Based on their results, they proposed a new type of the fin surface pattern with a wave located only in the upstream part (fin B). Then, they presented the comparison of the new fin pattern with the whole wavy fin (fin A) and whole plain plate fin (fin C). The results showed that within the range of the Reynolds number studied, the Nusselt number for fin B was only about 4% lower than for fin A and about 45% higher than for fin C while the friction factor of fin B was about 18% lower than for fin A and only about 26% higher than for fin C. The comparison at the identical Re number showed that fin B had the best comprehensive performance among the three types of fins, followed by fin C and fin A. Within the range of the Reynolds number studied, compared to fin C, the increased percentage of Nu/f of fin B varied from 12.4% to 18.5%; compared to fin A, this percentage ranged from 14.9% to 20%. Also, It could be seen that under the identical pressure drop constraint, fin B had the best performance too, followed by fin A and fin C. Moreover, It could be seen that under the identical pumping power constraint, fin B had the similar performances to fin A, and both of them were superior to fin C.

Junqi et al. (2007) studied experimentally a total of 11 cross-flow heat exchangers having wavy fin and flat tube. They conducted a series of tests for air side Reynolds number in the range of 800–6500 with different fin pitches (2.0, 2.25 and 2.5 mm), fin lengths (43, 53 and 65 mm) and fin heights (7, 8 and 10 mm), at a constant tube-side water flow rate of 2.5 m^3/h. They analyzed the air side thermal performance data using the effectiveness-number of transfer units (NTU) method. They reported the characteristics of heat transfer and pressure drop for different geometry parameters in terms of Colburn j-factor and Fanning friction factor f, as a function of Reynolds number (Re). They examined the effects of fin pitch (S), fin height (S) and fin length (L_d) on the performance of heat transfer and pressure drop. They derived the general correlations for j and f factors by multiple linear regression analysis and *F* test of significance. Their correlation of the heat transfer performance of the wavy fins was:

$$j = 0.0836\mathrm{Re}^{-0.2309}\left(\frac{S}{H}\right)^{0.1284}\left(\frac{S}{2A}\right)^{-0.153}\left(\frac{L_d}{\lambda}\right)^{-0.326} \quad (7)$$

Their correlation of the frictional performance of the wavy fins was:

$$f = 1.16\mathrm{Re}^{-0.309}\left(\frac{S}{H}\right)^{0.3703}\left(\frac{S}{2A}\right)^{-0.25}\left(\frac{L_d}{\lambda}\right)^{-0.1152} \quad (8)$$

They claimed that their correlations for j and f factors could predict 95% of the experimental data within $\pm$10%.

Sheik Ismail et al. (2009) analyzed 3 typical compact plate-fin heat exchangers using Fluent software for quantification of flow maldistribution, caused by the orientation of inlet and outlet nozzles in the heat exchanger, effects on the heat exchanger performance with ideal and real cases. The authors modified the headers by providing suitable baffle plates for improvement in flow distribution. Also, they analyzed numerically 3 offset strip fin and 16 wavy fin geometries used in the compact plate-fin heat exchangers. Colburn factor j and Fanning friction factor f vs. Reynolds number *Re* design data were generated using CFD analysis only for turbulent flow region. For the validation of the numerical analysis conducted in their study, a rectangular fin geometry having same dimensions as that of the wavy fin had been analyzed. They compared the results of the wavy fin with the analytical results of a rectangular fin and found good agreement. Similarly, they compared the numerical results of offset strip fin with the correlations available in the open literature and found good agreement with most of the earlier findings.

Sheik Ismail et al. (2010) presented a review on the research and developments of compact offset and wavy plate-fin heat exchangers in terms of pressure drop and heat transfer characteristics. The authors summarized their review under three major sections. They were offset fin characteristics, wavy fin characteristics and non-uniformity of the inlet fluid flow. They compared and summarized the different research aspects relating to internal single phase flow studied in offset and wavy fins by the previous researchers. Moreover, they addressed the works done on the non-uniformity of this fluid flow at the inlet of the compact heat exchangers and compared the methods available to minimize these effects.

3. PROPOSED METHODOLOGY

The proposed research considers the analytical modeling of complex internal flows for wavy fins. The approach taken to developing a robust model is to use fundamental theory of heat transfer and fluid dynamics. The process applied to these problems is threefold. First, asymptotic and scaling principles are used to determine the limiting behavior of the flow phenomena of interest. Second, simple theoretical models are developed using fundamental theory to link the asymptotic characteristics through non-linear transitions. Such a model will be robust, since it will include geometric variables (H, S, A, and λ) and

Reynolds number (Re) and Prandtl number (Pr). This aspect has not been addressed in any of the literature. Further it is expected with more viscous fluids such as water and oil at low Reynolds numbers, that this characteristic is stronger than with air as a working fluid. Taking advantage of these special limiting properties enables the development of an analytically based model. Third, experimental and numerical data collected from the published literature are used to validate the models. This methodology was applied by Muzychka (1999) for the offset strip fin (OSF) system with air as a working fluid and in Muzychka and Kenway (2009).

3.1 Modeling the f and j Characteristics of Wavy Fin Geometry

Figure 2 shows basic cell of wavy fin geometry (a) characteristic dimensions of a wavy fin channel, and (b) top view of a wavy channel.

The wavy fin system is modeled assuming that it can be approximated as a sinusoidal wave. This allows the effective flow length to be determined which in turn leads to the enhanced surface area. Assuming a sinusoidal wave has an amplitude (A) and a wave length (λ). The equation of the sinusoidal wave is

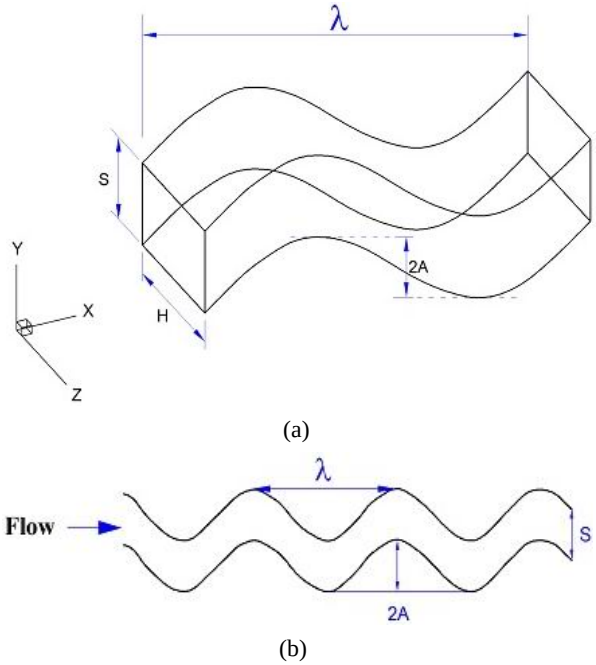

FIG. 2: Basic cell of wavy fin geometry: (a) characteristic dimensions of a wavy fin channel and (b) top view of a wavy channel.

$$f(x) = A\sin\left(\frac{2\pi x}{\lambda}\right) \tag{9}$$

The derivative of $f(x)$ is

$$f'(x) = \frac{2A\pi}{\lambda}\cos\left(\frac{2\pi x}{\lambda}\right) \tag{10}$$

The length of the sinusoidal wave (L_e) is

$$\begin{aligned} L_e &= 2\int_0^{\lambda/2}\sqrt{1+[f'(x)]^2}dx \\ &= 2\int_0^{\lambda/2}\sqrt{1+\left[\frac{2A\pi}{\lambda}\cos\left(\frac{2\pi x}{\lambda}\right)\right]^2}dx \end{aligned} \tag{11}$$

Using Maple software, we obtain

$$L_e = 2\frac{\sqrt{\lambda^2+4A^2\pi^2}}{\pi}E\left(\frac{2A\pi}{\sqrt{\lambda^2+4A^2\pi^2}}\right) \tag{12}$$

where $E(\cdot)$ is the complete elliptic integral of the second kind. We can define the wavy-fin-channel corrugation ratio (γ) as:

$$\gamma = \frac{2A}{\lambda} \tag{13}$$

Substituting Eq. (13) into Eq. (12), we obtain

$$L_e = 2\lambda\frac{\sqrt{1+\gamma^2\pi^2}}{\pi}E\left(\frac{\gamma\pi}{\sqrt{1+\gamma^2\pi^2}}\right) \tag{14}$$

and the ratio of the length of the sinusoidal wave (L_e) to the wavy fin wavelength (λ) is

$$\frac{L_e}{\lambda} = 2\frac{\sqrt{1+\gamma^2\pi^2}}{\pi}E\left(\frac{\gamma\pi}{\sqrt{1+\gamma^2\pi^2}}\right) \tag{15}$$

From Eq. (15), the ratio (L_e/λ) approaches unity when ($\gamma \to 0$), i.e., when waviness is small or not present. The elliptic integral can be solved for in most mathematical software or using handbook approximations.

3.2 Low Reynolds Number Asymptote

Shah and London (1978) gave the following relation for (fRe) for laminar flow forced convection in rectangular ducts as a function of the aspect ratio (α):

$$\begin{aligned} f\mathrm{Re} = 24(1 &- 1.3553\alpha + 1.9467\alpha^2 - 1.7012\alpha^3 \\ &+ 0.9564\alpha^4 - 0.2537\alpha^5) \end{aligned} \tag{16}$$

$$\alpha = \frac{S}{H} \tag{17}$$

At low Reynolds number, viscous forces dominate and the flow behavior is the same as that in rectangular ducts with the wavy surface simply providing a longer flow path or residence time. As a result, (fRe) for laminar flow forced convection in wavy fins is equal to (fRe) for laminar flow forced convection in rectangular ducts multiplied by the ratio of the length of the sinusoidal wave (L_e) to the wavy fin wavelength (λ). Thus, using Eqs. (15)–(17), we obtain:

$$f\mathrm{Re}_{\text{wavy}} = f\mathrm{Re}_{\text{channel}} \left(\frac{L_e}{\lambda} \right) \tag{18}$$

$$f\mathrm{Re}_{\text{wavy}} = 48 \frac{\sqrt{1+\gamma^2\pi^2}}{\pi} E\left(\frac{\gamma\pi}{\sqrt{1+\gamma^2\pi^2}} \right) (1 - 1.3553\alpha + 1.9467\alpha^2 - 1.7012\alpha^3 + 0.9564\alpha^4 - 0.2537\alpha^5) \tag{19}$$

where γ and α were defined in Eqs. (13) and (17) respectively.

For the Nusselt number (Nu), Shah and London (1978) gave the following relations for laminar flow forced convection in rectangular ducts at the uniform wall temperature boundary condition and the uniform heat flux boundary condition as a function of the aspect ratio (α)

$$\mathrm{Nu}_T = 7.541(1 - 2.610\alpha + 4.970\alpha^2 - 5.119\alpha^3 + 2.702\alpha^4 - 0.548\alpha^5) \tag{20}$$

$$\mathrm{Nu}_{H1} = 8.235(1 - 2.0421\alpha + 3.0853\alpha^2 - 2.4765\alpha^3 + 1.0578\alpha^4 - 0.1861\alpha^5) \tag{21}$$

where α was defined in Eq. (17).

The Nusselt number (Nu) for laminar flow forced convection in wavy fins at the uniform wall temperature boundary condition and the uniform heat flux boundary condition will be the same definition in Eqs. (20) and (21) as they are assumed to be based on total surface area and not nominal surface area.

The Colburn j factor is defined as:

$$j = \mathrm{StPr}^{2/3} = \frac{\mathrm{Nu}}{\mathrm{RePr}^{1/3}} \tag{22}$$

3.3 Laminar Boundary Layer (LBL) Asymptote

As the Reynolds number increases, multiple pairs of counter-rotating helical vortices are created that result in a higher momentum and energy transport. In the entrance region where the boundary layer thickness is small, the results are similar for all different shapes of ducts. Shapiro et al. (1954) derived an analytical result for the apparent friction factor in the entrance region of the circular duct using several methods. The leading term in the solution using the characteristic length D_h is given by

$$f_{\text{app}}\mathrm{Re}_{D_h} = \frac{3.44}{\sqrt{L^+}} \quad L^+ = L/(D_h\mathrm{Re}_{D_h}) < 0.001 \tag{23}$$

This solution does not depend on the duct shape and can be used to compute the apparent friction factor in the entrance region of most ducts and channels.

For the laminar boundary layer, the Nusselt number (Nu) is given by

$$\mathrm{Nu}_L = 0.664\mathrm{Re}_L^{1/2}\mathrm{Pr}^{1/3} \tag{24}$$

Using Eqs. (22) and (24), we obtain:

$$j_{\text{LBL}} = \frac{0.664}{\mathrm{Re}_L^{1/2}} = \frac{0.664}{\mathrm{Re}_{D_h}^{1/2}} \left(\frac{D_h}{L} \right)^{1/2} \tag{25}$$

The length (L) in Eqs. (23) and (25) is the *half length of the sinusoidal wave* ($L \sim 0.5L_e$) because it is from the top to the bottom of the sinusoidal wave, i.e.

$$L = \frac{L_e}{2} = \lambda \frac{\sqrt{1+\gamma^2\pi^2}}{\pi} E\left(\frac{\gamma\pi}{\sqrt{1+\gamma^2\pi^2}} \right) \tag{26}$$

The hydraulic diameter (D_h) in Eqs. (23) and (25) is required in the calculations. The hydraulic diameter (D_h) in some references such as Kays and London (1984) is defined as four times the hydraulic radius (r_h) but in this work, the hydraulic diameter (D_h) is defined as:

$$D_h = \frac{4SH}{2(S+H)} = \frac{2S}{(\alpha+1)} \tag{27}$$

It is clear from Eq. (27) that the hydraulic diameter (D_h) is equal to two times the fin spacing ($D_h = 2S$) for two-dimensional flow ($\alpha \to 0$). If FPI is known, the fin spacing (in.) is the reciprocal of FPI. There is not much difference between the current definition of the hydraulic diameter (D_h) and the definition adopted by Kays and London (1984).

3.4 Asymptotic Model

The combined asymptotic model of the frictional performance of the wavy fins is:

$$f_{\text{asy}} = \left[(f_{\text{wavy}})^2 + (f_{\text{app}})^2 \right]^{1/2} \tag{28}$$

In Eq. (28), the first component of the right hand side (f_{wavy}) is calculated using Eq. (19) while the second component of the right hand side (f_{app}) is calculated using Eq. (23).

In the asymptotic model of the frictional performance of the wavy fins, Eq. (28), 2 is chosen as the value, which minimizes the root-mean-square (RMS) error, e_{RMS}, between the model predictions and the available data.

The asymptotic model of the heat transfer performance of the wavy fins at the uniform wall temperature boundary condition is

$$j_{\text{asy}} = \left[(j_{\text{wavy},T})^5 + (j_{\text{LBL}})^5 \right]^{1/5} \tag{29}$$

$$j_{\text{wavy},T} = \frac{7.541}{\text{RePr}^{1/3}}(1 - 2.610\alpha + 4.970\alpha^2 - 5.119\alpha^3 + 2.702\alpha^4 - 0.548\alpha^5) \tag{30}$$

The second component of the right hand side in Eq. (29) (j_{LBL}) is calculated using Eq. (25).

In the asymptotic model of the heat transfer performance of the wavy fins at the uniform wall temperature boundary condition, Eq. (29), 5 is chosen as the value, which minimizes the RMS error, e_{RMS}, between the model predictions and the available data.

The present model does not consider that the flow could develop over the total wavy fin channel length. By this, we are neglecting effect that the first few wavy periods have on the final flow. In periodic flow systems like the OSF and wavy fins, the flow takes 4–5 periods to stabilize into a recurring boundary layer flow which is then deemed "fully developed". Inherent in any correlation or model for f and j, is that sufficient length is present to dampen out the effect of the first 4–5 periods or rows.

In the present model, the transition from laminar to turbulent is acceptable to model only up to Re $\sim$ 3000 due to the nature of the data.

4. RESULTS AND DISCUSSION

Examples of the Fanning friction factor f and Colburn j factor in air cooled compact wavy fin heat exchangers at different values of the geometric variables obtained from the published literature are presented to show features of the asymptotes, asymptotic analysis and the development of the simple compact models. The following data sets will be used to validate the model: Kays and London (1984), Gschwind and Kottke (1999), Zhang (2005), and Junqi et al. (2007).

4.1 Comparison of the Present Asymptotic Model with Data

Figures 3–5 show comparisons of the present asymptotic f and j model with the 3 sets of data from Kays and London (1984) (11.44–3/8W, 11.5–3/8W, and 17.8–3/8W) at Re = 500–8000, 400–10000, and 600–5000, respectively. It is clear that at the lower Reynolds number (Re), j data fall under model predictions due to an experimental phenomena when air is used as a test fluid called

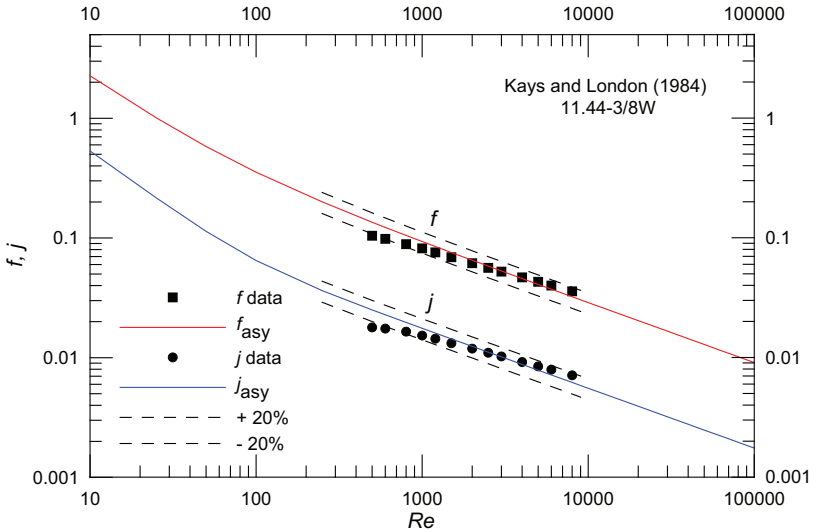

FIG. 3: Comparison of the present asymptotic f and j model with Kays and London's data (1984) (11.44–3/8 W).

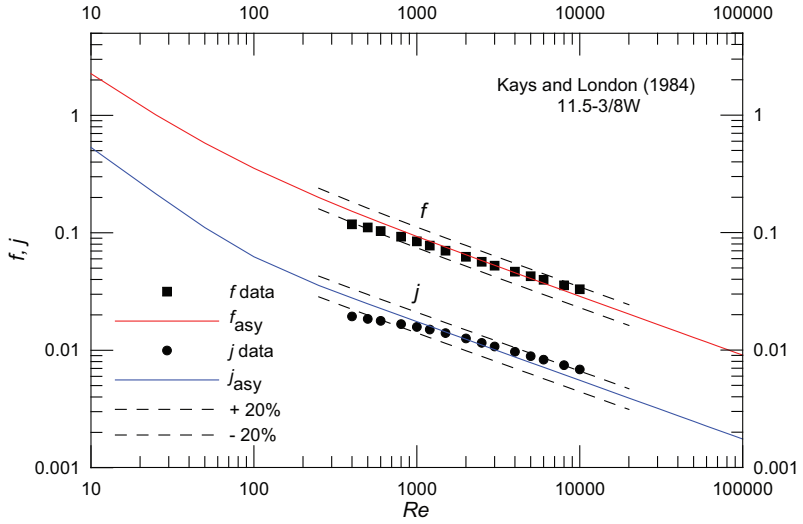

FIG. 4: Comparison of the present asymptotic f and j model with Kays and London's data (1984) (11.5–3/8 W).

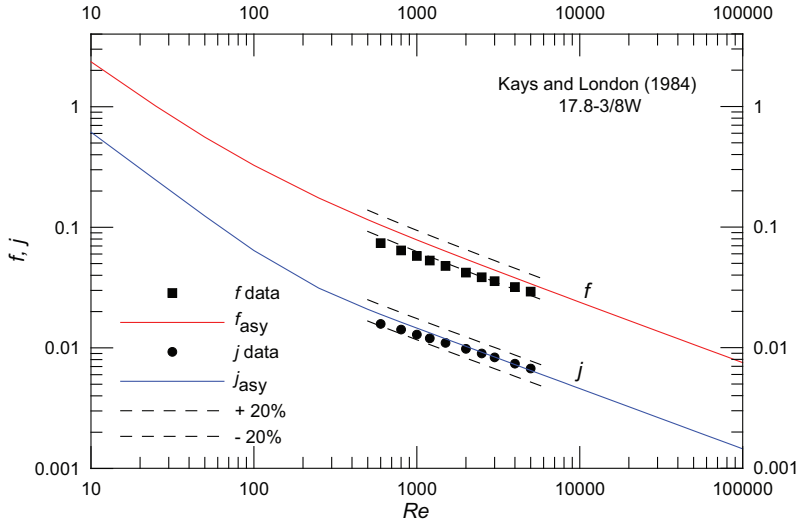

FIG. 5: Comparisons of the present asymptotic f and j model with Kays and London's data (1984) (17.8–3/8 W).

"roll over" as mentioned by Shah and Sekulic (2003). The RMS error, e_{RMS}, for f using Eq. (28) is equal to 13.75%, 12.70%, and 29.23%, respectively while the RMS error, e_{RMS}, for j using Eq. (29) is equal to 16.85%, 17.88%, and 9.69%, respectively.

Figure 6 shows comparison of the present asymptotic f model with Gschwind and Kottke's data (1999) for the sinusoidal wavy duct with constant wavelength (λ) = 26 mm, amplitude (A) = 1.825 mm, and the dimensionless wavelength (λ/A) = 14.25. The fin spacing (S) is equal to the amplitude (A) = 1.825 mm. The RMS error, e_{RMS}, for f using Eq. (28) is equal to 13.46%.

Figure 7 shows comparisons of the present asymptotic f and j model with numerical data of Zhang (2005) for steady forced convection heat transfer in three-dimensional wavy plate-fin channels in air flow (Pr = 0.7) in the laminar or low Reynolds number (Re) regime = 10–1000 for Case 3 (α = 0.373, γ = 0.2667, and ε = 0.470). The numerical data of Zhang (2005) is calculated at *Re* = 10, 25, 50, 100, 250, 500, 750, and 1000, respectively. The RMS error, e_{RMS}, for f and j using Eqs. (28), and (29) is equal to 25.23%, and 21.46%, respectively.

Figure 8 shows comparisons of the present asymptotic f and j model with numerical data of Zhang

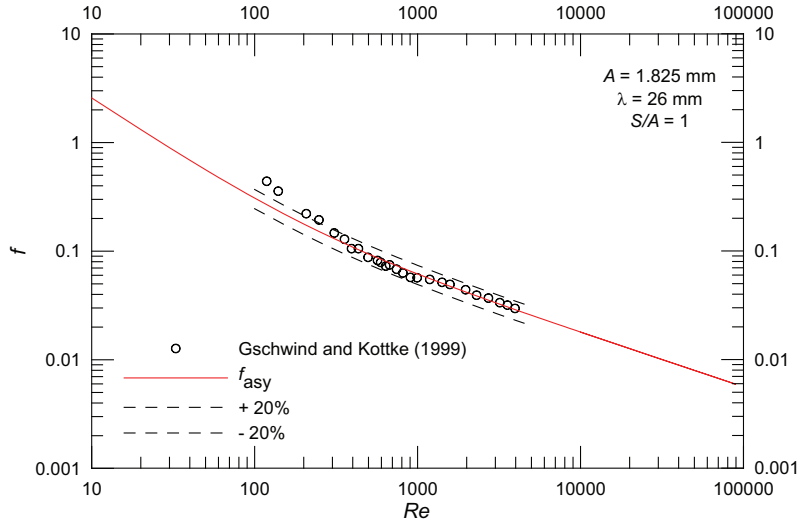

FIG. 6: Comparison of the present asymptotic f model with Gschwind and Kottke's data (1999) at $S/A = 1$.

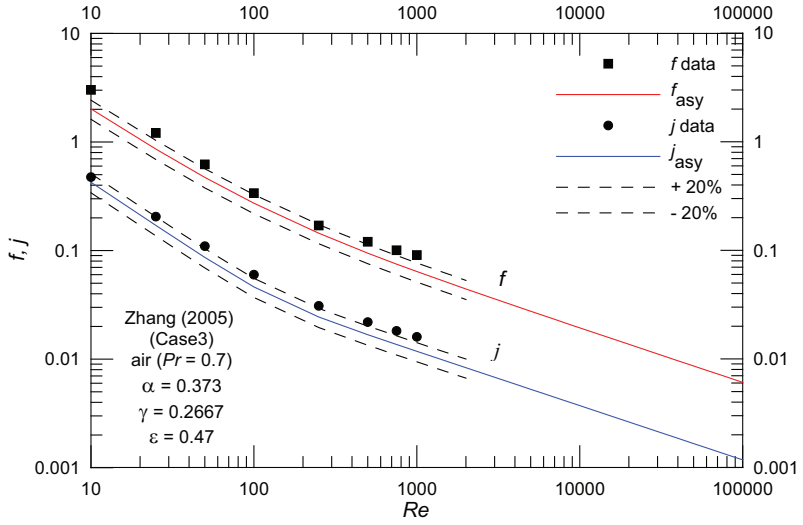

FIG. 7: Comparison of the present asymptotic f and j model with Zhang's data (2005) (Case 3).

(2005) for steady forced convection heat transfer in three-dimensional wavy plate-fin channels in air flow (Pr = 0.7) in the laminar or low Reynolds number (Re) regime = 10–1000 for Epsilon 2 ($\alpha = 0.968$, $\gamma = 0.2667$, and $\varepsilon = 0.803$). The numerical data of Zhang (2005) is calculated at Re = 10, 25, 50, 100, 250, 500, 750, and 1000, respectively. The RMS error, e_{RMS}, for f and j using Eqs. (28), and (29) is equal to 24.42%, and 11.93%, respectively.

Figure 9 shows comparisons of the present asymptotic f and j model with numerical data of Zhang (2005) for steady forced convection heat transfer in three-dimensional wavy plate-fin channels in air flow (Pr = 0.7) in the laminar or low Reynolds number (Re) regime = 10–1000 for Alpha 3 ($\alpha = 0.264$, $\gamma = 0.2667$, and $\varepsilon = 0.803$). The numerical data of Zhang (2005) is calculated at Re = 10, 25, 50, 100, 250, 500, 750, and 1000, respectively. The RMS error, e_{RMS}, for f and j using Eqs. (28), and (29) is equal to 24.48%, and 14.11%, respectively.

Figure 10 shows comparisons of the present asymptotic f and j model with numerical data of Zhang (2005) for steady forced convection heat transfer in three-dimensional wavy plate-fin channels in air flow (Pr = 0.7) in the laminar or low Reynolds number (Re) regime = 10–1000 for Gamma 3 ($\alpha = 0.637$, $\gamma = 0.1333$, and $\varepsilon = 0.803$).

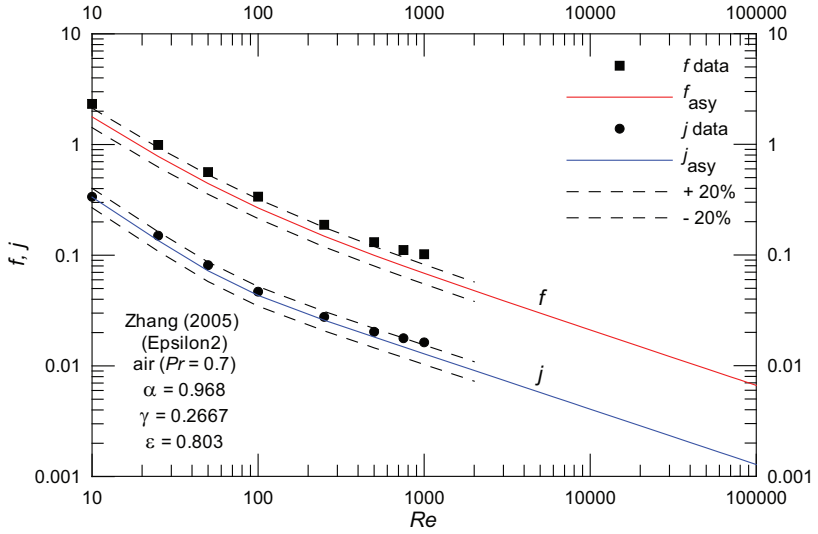

FIG. 8: Comparison of the present asymptotic f and j model with Zhang's data (2005) (Epsilon 2).

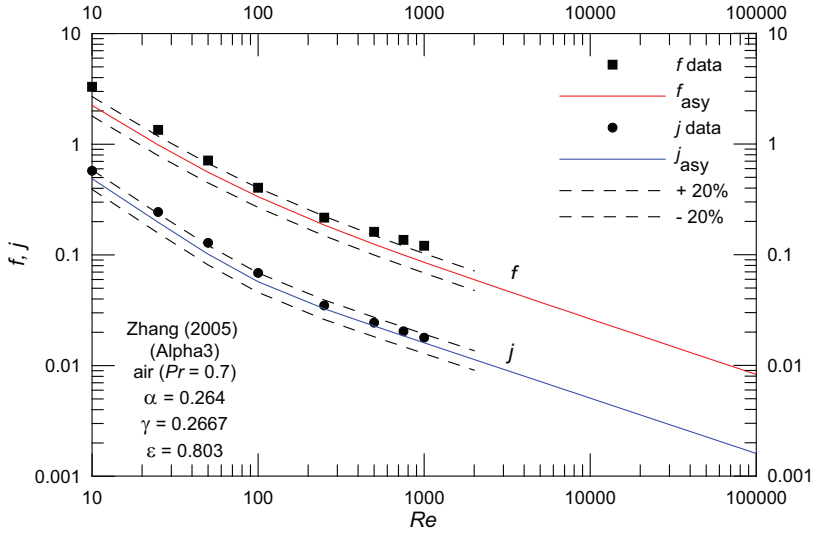

FIG. 9: Comparison of the present asymptotic f and j model with Zhang's data (2005) (Alpha 3).

The numerical data of Zhang (2005) is calculated at Re = 10, 25, 50, 100, 250, 500, 750, and 1000, respectively. The RMS error, e_{RMS}, for f and j using Eqs. (28), and (29) is equal to 34.82%, and 10.15%, respectively.

Figure 11 shows comparisons of the present asymptotic f and j model with Junqi et al.'s data (2007) and their correlations, Eqs. (8), and (7), respectively for S = 2.0 mm, H = 10.0, and L_d = 43.0 mm. The RMS error, e_{RMS}, for f and j using Eqs. (28), and (29) the present asymptotic f and j model is equal to 15.00%, and 50.30%, respectively while the RMS error, e_{RMS}, for f and j using Eqs. (8) and (7) is equal to 18.12%, and 3.20%, respectively. We think the main reasons for the difference are that the profiles of wavy fins are not identical to those of Junqi et al. (2007). The wavy fins' profiles in the present study are sinusoidal however the Junqi et al.'s wavy fin profiles are the triangular profiles with round corners. Also, Junqi et al.'s data/correlations (2007) of f and j factor do not agree with the Kays and London's data (1984) based on two wavy fins that are named 11.4–3/8 W and 11.5–3/8 W and that it appears that Junqi et al. (2007) used a more triangular waveform.

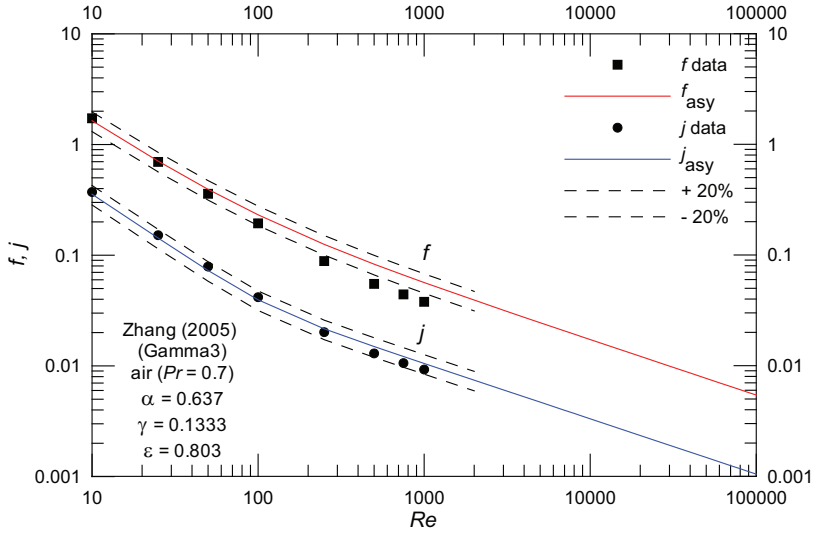

FIG. 10: Comparison of the present asymptotic f and j model with Zhang's data (2005) (Gamma 3).

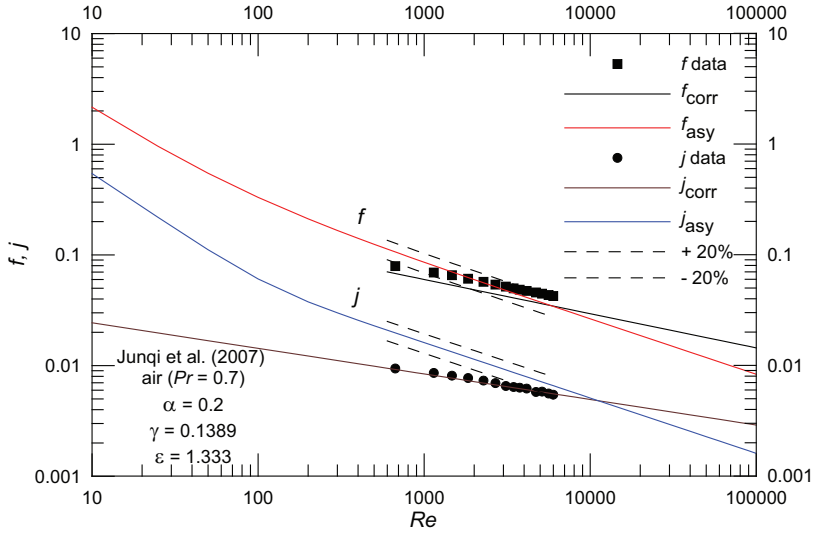

FIG. 11: Comparison of the present asymptotic f and j model with Junqi et al.'s data (2007) at S = 2.0, H = 10.0, and L_d = 43.0 mm.

Table 1 gives summary of model and data comparisons.

5. SUMMARY AND CONCLUSIONS

New models for predicting pressure drop and heat transfer in air cooled compact wavy fin heat exchangers are proposed, based upon an asymptotic modeling method. These new models are developed by combining the asymptotic behavior for the low Reynolds number and laminar boundary layer regions. Models in these two regions are developed by taking into account the geometric variables like: fin height (H), fin spacing (S), wave amplitude (A), fin wavelength (λ), Reynolds number (Re), and Prandtl number (Pr). The new models for f and j cover a wide range of Reynolds number = 10–10000. It can be seen that the present model represents the different data sets available in the published literature at different values of the geometric variables in a successful manner. The present model is quite accurate given the uncertain-

TABLE 1: Summary of model and data supplied comparison

Kays and London's data (1984)

H, in	FPI, in^{-1}	t, in	L, in	A, in	Pr	Re	f, %rms	j, %rms
0.413	11.44	0.006	0.375	0.08	0.7	500-8000	13.75%	16.85%
0.375	11.5	0.01	0.375	0.08	0.7	400-10000	12.70%	17.88%
0.413	17.5	0.006	0.375	0.08	0.7	600-5000	29.23%	9.69%

Experimental Fanning friction factor f data of Gschwind and Kottke (1999)

Wavy amplitude (A)	**Wavelength** (λ)	(S)	e_{RMS} f_{asy}
1.825	26	1.825	13.46%
1.825	26	2.7375	13.81%
1.825	26	3.65	13.90%
1.825	26	4.5625	17.41%
1.825	26	5.475	26.78%

Numerical data of Zhang (2005), Pr = 0.7

Cases	**Fin spacing** (S)	**Fin height** (H)	**Wavy length** (λ)	**Amplitude** (A)	α $(=S/H)$	γ $(=2A/\lambda)$	ε $(=S/2A)$	e_{RMS} f_{asy}	e_{RMS} j_{asy}
Case 1	0.122	0.126	0.375	0.05	0.968	0.2667	1.220	34.28%	8.30%
Case 2	0.0803	0.126	0.375	0.05	0. 637	0.2667	0.803	26.01%	13.33%
Case 3	0.0470	0.126	0.375	0.05	0.373	0.2667	0.470	25.23%	21.46%
Case 4	0.0303	0.126	0.375	0.05	0.240	0.2667	0.303	24.42%	23.57%
Epsilon 1	0.122	0.126	0.375	0.05	0.968	0.2667	1.220	34.28%	8.30%
Epsilon 2	0.0803	0.0826	0.375	0.05	0.968	0.2667	0.803	24.42%	11.93%
Epsilon 3	0.0470	0.0486	0.375	0.05	0.968	0.2667	0.470	25.49%	21.27%
Epsilon 4	0.0303	0.0313	0.375	0.05	0.968	0.2667	0.303	24.72%	24.53%
Alpha 1	0.0803	0.0803	0.375	0.05	1.000	0.2667	0.803	30.08%	16.16%
Alpha 2	0.0803	0.126	0.375	0.05	0. 637	0.2667	0.803	26.01%	13.33%
Alpha 3	0.0803	0.304	0.375	0.05	0.264	0.2667	0.803	24.48%	14.11%
Alpha 4	0.0803	0.482	0.375	0.05	0.167	0.2667	0.803	25.10%	16.17%
Gamma 1	0.1606	0.252	0.375	0.1	0. 637	0.5333	0.803	76.96%	42.25%
Gamma 2	0.0803	0.126	0.375	0.05	0. 637	0.2667	0.803	26.01%	13.33%
Gamma 3	0.0803	0.126	0.75	0.05	0. 637	0.1333	0.803	34.82%	10.15%
Gamma 4	0.0803	0.126	1.5	0.05	0. 637	0.0667	0.803	45.73%	5.95%

ties in heat exchanger core manufacture, and also that it captures the trends in the data quite well even when the RMS errors are larger, i.e. they are biased or offset errors.

ACKNOWLEDGMENTS

The authors acknowledge the support of the Natural Sciences and Engineering Research Council of Canada (NSERC) and TAT Technologies Inc.

REFERENCES

Ali, M. M. and Ramadhyani, S., Experiments on convective heat transfer in corrugated channels, *Exp. Heat Transfer*, vol. **5**, no. 3, pp. 175–193, 1992.

Amano, R. S., A numerical study of laminar and turbulent heat transfer in a periodically corrugated wall channel, *ASMEJ. Heat Transfer*, vol. **107**, no. 3, pp. 564–569, 1985.

Amano, R. S., Bagherlee, A., Smith, R. J., and Niess, T. G., Turbulent Heat Transfer in Corrugated Wall Channels with and without Fins, *ASMEJ. Heat Transfer*, vol. **109**, no. 1, pp.

62–67, 1987.

Asako, Y. and Faghri, M., Finite-volume solutions for laminar flow and heat transfer in a corrugated duct, *ASMEJ. Heat Transfer*, vol. **109**, no. 3, pp. 627–634, 1987.

Asako, Y., Nakamura, H., and Faghri, M., Heat transfer and pressure drop characteristics in a corrugated duct with rounded corners, *Int. J. Heat Mass Transfer*, vol. **31**, no. 6, pp. 1237–1245, 1988.

Goldstein, L. and Sparrow, E. M., Heat/mass transfer characteristics for flow in a corrugated wall channel, *ASME J. Heat Transfer*, vol. **99**, no. 2, pp. 187–195, 1977.

Gschwind, P. and Kottke, V., Heat and Mass Transfer of Free-Flow Arrangements with Corresponding Pressure Drop, in: R. K. Shah (Ed.), *Compact Heat Exchangers and Enhancement Technology for the Process Industries*, New York: Begell House, 1999.

Junqi, D., Jiangping, C., Zhijiu, C., Yimin, Z., and Wenfeng, Z., Heat transfer and pressure drop correlations for the wavy fin and flat tube heat exchangers, *Appl. Thermal Eng.*, vol. **27**, no. 11–12, pp. 2066–2073, 2007.

Kays, W. M. and London, A. L., *Compact Heat Exchangers*, 3rd ed., Kreiger Publishing, Melbourne, FL., 1984.

Lin, Y.-T., Hwang, Y.-M., and Wang, C.-C., Performance of the herringbone wavy fin under dehumidifying conditions, *Int. J. Heat Mass Transfer*, vol. **45**, no. 25, pp. 5035–5044, 2002.

Manglik, R. M., Zhang, J., and Muley, A., Low Reynolds number forced convection in three-dimensional wavy-plate-fin compact channels: fin density effects, *Int. J. Heat Mass Transfer*, vol. **48**, no. 8, pp. 1439–1449, 2005.

Metwally, H. M. and Manglik, R. M., A computational study of enhanced heat transfer in laminar flows of non-Newtonian fluids in corrugated-plate channels, in: R. M. Manglik et al. (Eds.), *Advances in Enhanced Heat Transfer*, HTD-vol. **365**/PID-vol. **4**, pp. 41–48, 2000.

Mulay, A., Borghese, J., Manglik, R. M., and Kundu, J., Experimental and numerical investigation of thermal-hydraulic characteristics of wavy-channel compact heat exchanger, *Proc. 12^{th} Int. Heat Transfer Conf.*, France, vol. **4**, pp. 417–422, 2002.

Muley, A., Borghese, J. B., White, S. L., and Manglik, R. M., Enhanced thermal-hydraulic performance of a wavy-plate-fin compact heat exchanger: effect of corrugation severity, *Proc. 2006 ASME Int. Mechanical Engineering Congress and Exposition (IMECE2006)*, Chicago, IL, USA, IMECE2006-14755, 2006.

Muzychka, Y. S., *Analytical and Experimental Study of Fluid Friction and Heat Transfer in Low Reynolds Number Flow Heat Exchangers*, Ph.D. Thesis, University of Waterloo, 1999.

Muzychka, Y. S. and Kenway, G., A model for the thermal hydraulic characteristics of the offset strip fin array for large Prandtl number liquids, *J. Enhanced Heat Transfer*, vol. **16**, no. 1, pp. 73–92, 2009.

O'Brien, J. E. and Sparrow, E. M., Corrugated duct heat transfer, pressure drop, and flow visualization, *ASME J. Heat Transfer*, vol. **104**, no. 3, pp. 410–416, 1982.

Rush, T. A., Newell, T. A., and Jacobi, A. M., An experimental study of flow and heat transfer in sinusoidal wavy passages, *Int. J. Heat Mass Transfer*, vol. **42**, no. 9, pp. 1541–1553, 1999.

Shah, R. K. and London, A. L., *Advances in Heat Transfer,* Suppl. 1, *Laminar Forced Flow Convection in Ducts*, New York: Academic Press, 1978.

Shah, R. K. and Sekulic, D., *Fundamentals of Heat Exchanger Design*: Wiley, Hoboken, NJ, 2003.

Shapiro, A. H., Siegel, R., and Kline, S. J., Friction factor in the laminar entry region of a smooth tube, *Proc. 2^{nd} U.S. Nat. Congress of Applied Mechanics*, pp. 733–741, 1954.

Sheik Ismail, L., Ranganayakulu, C., and Shah, R. K., Numerical study of flow patterns of compact plate-fin heat exchangers and generation of design data for offset and wavy fins, *Int. J. Heat Mass Transfer*, vol. **52**, no. 17–18, pp. 3972–3983, 2009.

Sheik Ismail, L., Velraj, R., and Ranganayakulu, C., Studies on pumping power in terms of pressure drop and heat transfer characteristics of compact plate-fin heat exchangers—A review, *Renewable Sustainable Energy Rev.*, vol. **14**, no. 1, pp. 478–485, 2010.

Sparrow, E. M. and Comb, J. W., Effect of interwall spacing and fluid flow inlet conditions on a corrugated-wall heat exchanger, *Int. J. Heat Mass Transfer*, vol. **26**, no. 7, pp. 993–1005, 1983.

Sparrow, E. M. and Hossfeld, L. M., Effect of rounding of protruding edges on heat transfer and pressure drop in a duct, *Int. J. Heat Mass Transfer*, vol. **27**, no. 10, pp. 1715–1723, 1984.

Tao, Y. B., He, Y. L., Wu, Z. G., and Tao, W. Q., Numerical design of an efficient wavy fin surface based on the local heat transfer coefficient study, *J. Enhanced Heat Transfer*, vol. **14**, no. 4, pp. 315–322, 2007.

Vyas, S., Zhang, J., and Manglik, R. M., Steady recirculation and laminar forced convection in a sinusoidal wavy channel, *ASME J. Heat Transfer*, vol. **126**, no. 4, p. 500, 2004.

Webb, R. and Kim, N.-H., *Principles of Enhanced Heat Transfer*, 2nd ed.: Taylor and Francis, New York, NY, 2005.

Zhang, J., *Numerical Simulations of Steady Low-Reynolds-Number Flows and Enhanced Heat Transfer in Wavy Plate-Fin Passages*, Ph.D. thesis, University of Cincinnati, 2005.

Zhang, J., Kundu, J., and Manglik, R. M., Effect of fin waviness

and spacing on the lateral vortex structure and laminar heat transfer in wavy-plate-fin cores, *Int. J. Heat Mass Transfer*, vol. **47**, no. 8–9, pp. 1719–1730, 2004.

Zhang, J., Muley, A., Borghese, J. B., and Manglik, R. M., Computational and experimental study of enhanced laminar flow heat transfer in three-dimensional sinusoidal wavy-plate-fin channels, *Proc. ASME Summer Heat Transfer Conf.*, vol. **1**, pp. 665–672, 2003.